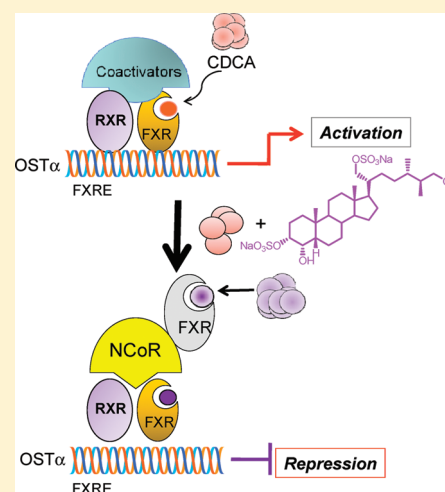


Discovery of Sulfated Sterols from Marine Invertebrates as a New Class of Marine Natural Antagonists of Farnesoid-X-Receptor

Valentina Sepe,[†] Giuseppe Bifulco,[‡] Barbara Renga,[§] Claudio D'Amore,[§] Stefano Fiorucci,^{§,||} and Angela Zampella^{*,†,||}[†]Dipartimento di Chimica delle Sostanze Naturali, Università di Napoli "Federico II", via D. Montesano 49, 80131 Napoli, Italy[‡]Dipartimento di Scienze Farmaceutiche, Università di Salerno, via Ponte don Melillo, 84084 Fisciano (SA), Italy[§]Dipartimento di Medicina Clinica e Sperimentale, Università di Perugia, Nuova Facoltà di Medicina e Chirurgia, Via Gerardo Dottori no. 1 S. Andrea delle Fratte, 06132 Perugia, Italy

ABSTRACT: We report the biochemical characterization of sulfated polyhydroxy sterols isolated from marine invertebrates as potent antagonists of farnesoid-X-receptor (FXR), a ligand-regulated transcription factor involved in the regulation of lipid and glucose homeostasis in mammals. Molecular characterization of a library of sulfated polyhydroxysteroids resulted in the identification of a first FXR antagonist. In contrast to partial antagonists, this compound was endowed with an antagonistic activity on the expression of a subset of FXR-regulated genes in liver cells and abrogated the release of nuclear coreceptor from the promoter of these genes. The putative binding mode to FXR, obtained through docking calculations, suggested the crucial role played by the bent shape of the molecule as well as the presence of one hydroxyl group in its side chain. This compound is a major tool to explore the effect of FXR inhibition in pharmacological settings.



INTRODUCTION

The farnesoid-X-receptor (FXR, NR1H4) is an adopted member of the metabolic nuclear receptors (NRs) superfamily, highly expressed in liver, intestine, kidney, and adrenals.^{1–3} Shortly after its discovery, specific bile acids (BAs) were identified^{1–3} as endogenous ligands. In contrast to other endogenous steroids, BAs nucleus adopts a bent shape due to the A/B cis ring juncture that forces ring A to lie outside of the plane of the BCD ring system. As a result, the separation between the 3 α -OH and the C-24 carboxylate of 3 α ,7 α -dihydroxy-5 β -cholanic acid, chenodeoxycholic acid (CDCA), is substantially shorter than the contour length of the molecule (14 vs 21 Å). These features as well as the α -orientation of the hydroxyl group at position 3 give to BAs a profile that allows close fitting in the FXR pocket.⁴

Recent advances in FXR biology support the notion that this receptor represents a valuable pharmacological target.^{5–9} However, activation of FXR leads to complex responses that integrate beneficial actions and potentially undesirable side effects,^{5–9} the most relevant of which is the inhibition of BAs synthesis through the indirect repression of the expression of cytochrome 7A1 (Cyp7A1), the rate-limiting enzyme of this pathway. Furthermore, in liver cells, FXR represses the expression of basolateral transporters such as the multidrug resistance protein (MRP)-4, an ATP binding protein, serving the

basolateral excretion of BAs, a pathway that is protective in cholestasis, a set of liver disorders characterized by accumulation of BAs. Thus, the identification of selective FXR modulators targeting specific cluster of genes or FXR antagonists might have pharmacological relevance.^{5–9}

While several steroidal and nonsteroidal FXR ligands have been so far synthesized (Figure 1),^{10–13} only few natural FXR modulators have been described including guggulsterone, the active components of the resin extract of the tree *Commiphora mukul*,^{14,15} xanthohumol,¹⁶ the principal prenylated chalcone from beer hops, and some scalarane sesterterpenes isolated from a marine sponge.¹⁷ Indeed, guggulsterone, initially described as an FXR antagonist,^{18,19} was then proved to be a partial FXR agonist.²⁰ Although guggulsterone exerts antagonistic effects on FXR-induced recruitment of Src-1, it also induces the expression of the bile salt export pump (BSEP) transporter, a known FXR-regulated gene. In addition, guggulsterone is a rather promiscuous ligand²¹ interacting with the glucocorticoid, the progesterone and the pregnane-X-receptor (PXR). Therefore, despite a plausible mechanism of action via FXR, guggulsterone cannot be considered an FXR antagonist.

Received: October 15, 2010

Published: February 10, 2011

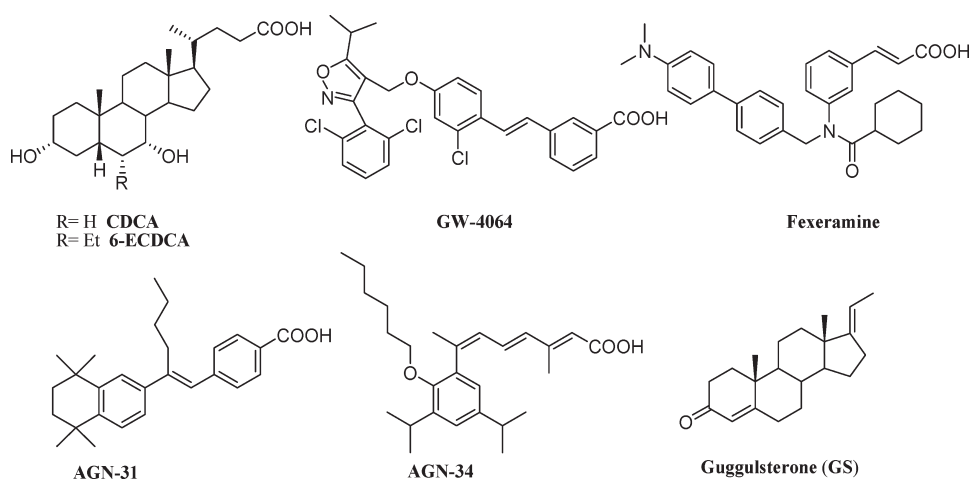


Figure 1. Recent examples of FXR modulators.

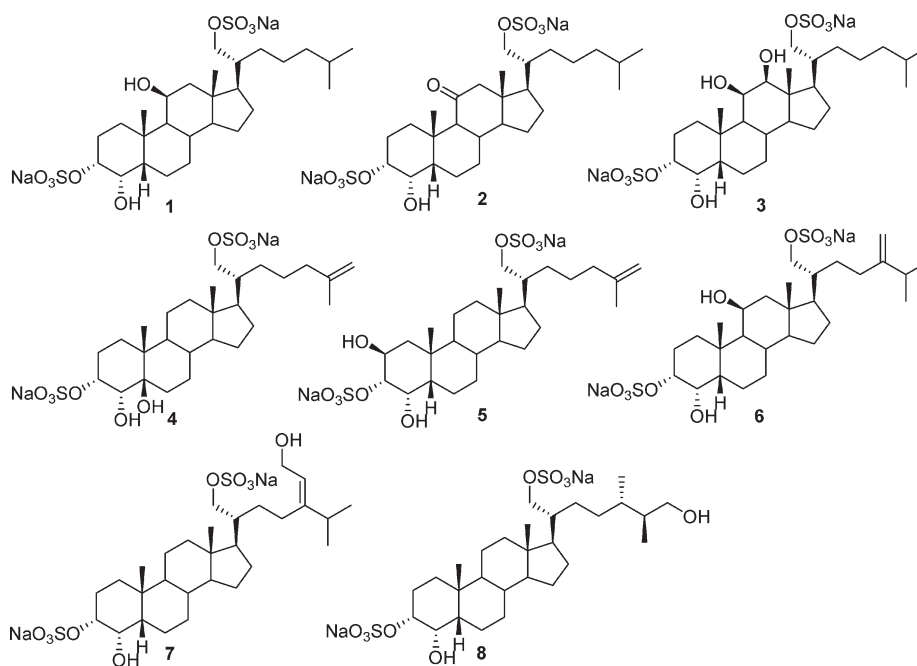


Figure 2. Selected sulfated steroids from marine ophiuroids.

As a part of our continuing research directed toward the discovery of marine natural NRs ligands, we have investigated a library of sulfated sterols isolated from marine echinoderms (Figure 2). Among echinoderms, ophiuroids (commonly known as brittle stars) have been proved a rich source of sulfated polyhydroxysterols endowed with biological activities including antiviral effects^{22–25} and action on specific enzymatic targets.²⁶

Apart from few exceptions, invariably, ophiuroid sterols show the presence of two sulfate groups located at C-3 and C-21 and the rare A/B cis ring junction, whereas the structural modifications relate to the presence of additional OH groups in rings A or D and to the complexity of side chain. Ophiuroid sterols share with BAs some key structural features: the presence of the A/B cis ring junction, the negative charge on the side chain, and the presence of polar groups in the α -position on ring A. These characteristics, recognized as key structural features for BAs activation of FXR, prompted us to investigate their capability to act as FXR modulators.

RESULTS AND DISCUSSION

Eight sulfated sterols, previously isolated from different collections of *Ophiocoma dentata*²⁷ (compounds 1 and 6), *Ophiarthrum elegans*²⁷ (compound 2), *Ophioderma longicaudum*²⁸ (compound 3), and *Ophiolepis superba*²⁹ (compounds 4, 5, 7, and 8) were selected. As shown in Figure 2, these compounds, all possessing 3 α ,21-disulfoxy-4 α -hydroxysubstituents and the A/B cis ring junction, could be divided into two broad structural classes: sterols with rather simple side chains (1–5) and sterols with branched side chains (6–8). The compounds belonging to first category show a lanosterol type side chain but differ for the hydroxylation pattern of rings A and C. The side chain of compounds 6–8 varies from a simple C-24 substituted (6) to more complex branched side chains with one additional polar OH group (7 and 8).

All of compounds were tested *in vitro*, using an hepatocarcinoma cell line (HepG2 cells) transfected with FXR, RXR, and

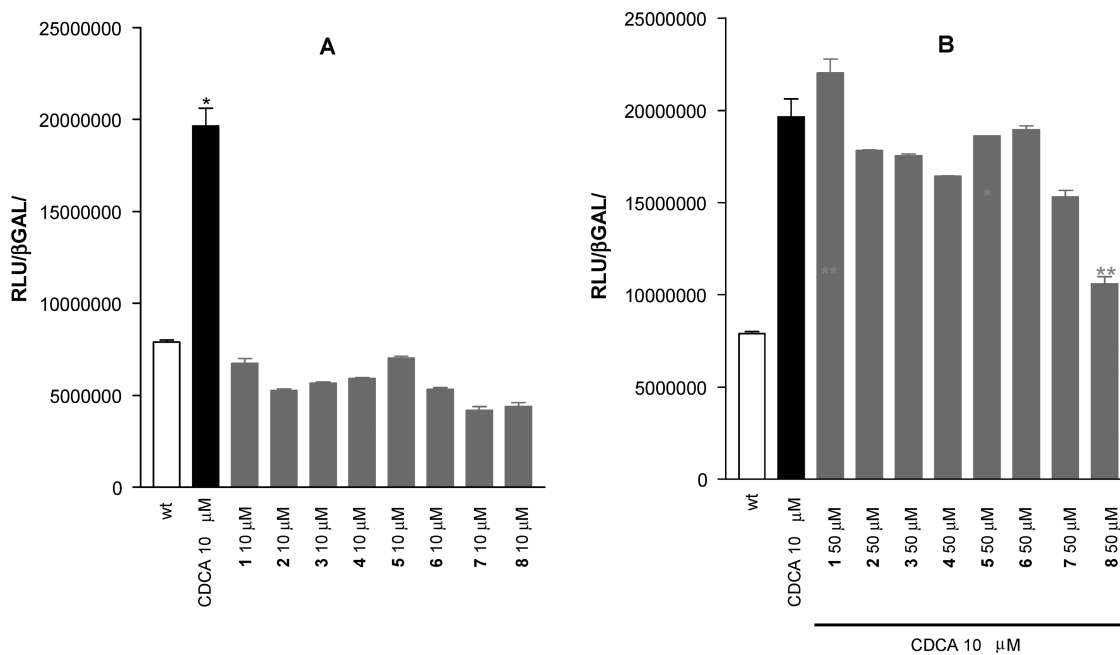


Figure 3. Luciferase reporter assay performed in HepG2 transiently transfected with pSG5FXR, pSG5RXR, pCMV-βgal, and p(hsp27)TKLUC vectors and stimulated 18 h with (A) 10 μM CDCA and 10 μM individual compounds 1–8 and (B) 10 μM CDCA alone or in combination with 50 μM compounds 1–8.

β-galactosidase expression vectors (pSG5FXR, pSG5RXR, and pCMV-βgal) and with p(hsp27)TKLUC reporter vector that contains the promoter of the FXR target gene heat shock protein 27 (hsp27) cloned upstream of the Luciferase gene.

HepG2 cells were stimulated with 10 μM compounds 1–8 with or without 10 μM CDCA. As shown in Figure 3A, despite the resemblance of their molecular shape with that of BAs, none of these compounds appears to be an FXR agonist in the transactivation assay.

However, when HepG2 cells transfected with FXR vectors were treated with compounds 1–8 (Figure 3B) in the presence of 10 μM CDCA, all compounds, with the exception of 1, showed a slight inhibitory activity against FXR transactivation, with compound 8 exhibiting a potent antagonist activity resulting in ≈80% inhibition of FXR transactivation induced by CDCA. This effect was concentration dependent, and, as shown in Figure 4, at a concentration of 100 μM, compound 8 almost completely reversed the effect exerted by CDCA on FXR expression (Figure 4, **P* < 0.05 vs CDCA alone).

To give support to the potential FXR antagonist activity of compound 8, we then tested its effects on the expression of genes that are targeted by CDCA in a FXR-dependent manner. Results shown in Figure 5 demonstrate that compound 8 inhibits the expression of canonical FXR target genes such as organic solute transporter α (OSTα) and organic solute transporter β (OSTβ) and BSEP.

Interestingly, the antagonistic activity of compound 8 was also observed for the Cyp7α1 gene, that is, negatively regulated by FXR in a SHP-dependent manner. Altogether, these data indicate that we have identified compound 8 as a potent and selective FXR antagonist. Furthermore, compound 8 differs from guggulsterone because this agent antagonizes the effects of FXR ligands on Cyp7α1 but induces BSEP. In contrast, compound 8 antagonizes FXR activity in both FXR up-regulated and down-regulated target genes.

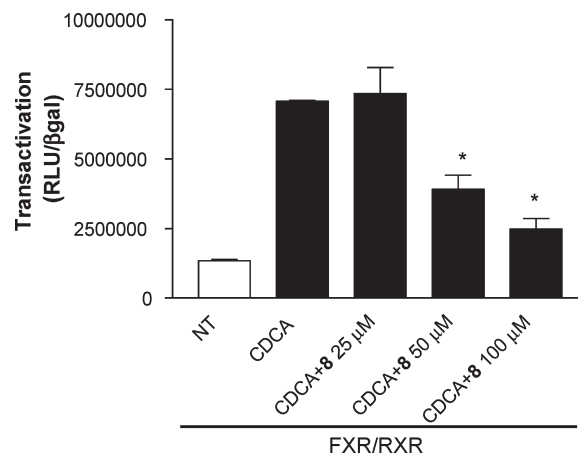


Figure 4. Concentration–response effect of compound 8 on of FXR transactivation induced by CDCA. The luciferase reporter assay was carried out in HepG2 transiently transfected with pSG5FXR, pSG5RXR, pCMV-βgal, and p(hsp27)TKLUC vectors and stimulated with 10 μM CDCA alone or in combination with increasing concentrations of compound 8. Data are means ± SEs of three experiments carried out in triplicate.

To gain further insights into the molecular mechanism mediating the antagonistic activity of compound 8, we then investigated the effect of this agent on a well-characterized corepressor of FXR, that is, the nuclear corepressor (NCoR). Because NCoR is released upon FXR binding to the promoter of target genes (see graphical abstract), an FXR antagonist would stabilize NCoR on the promoters of OST-α. Because stabilization of NCoR at the OSTα promoter would prevent its transcription, the results of this experiments would effectively provide a mechanistic explanation to the molecular mechanism of action of compound 8 on FXR. For this purpose, we have performed an experiment of

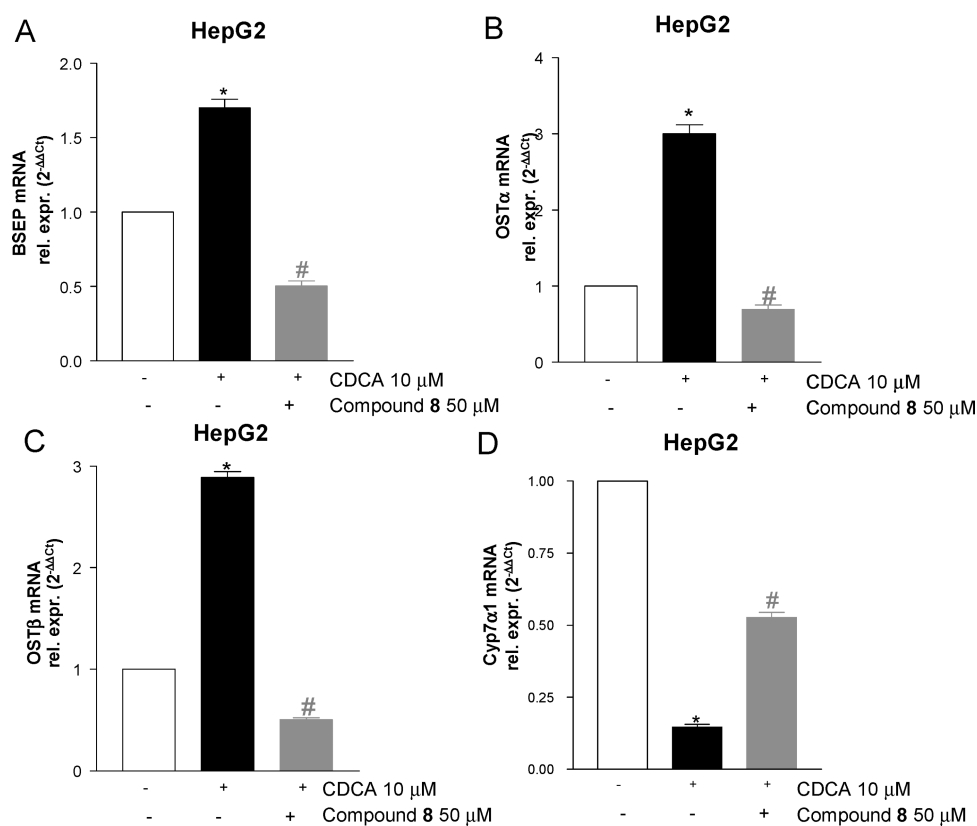


Figure 5. Real-time PCR of (A) BSEP, (B) OST α , (C) OST β , and (D) Cyp7 α 1 carried out on cDNA isolated from HepG2 not stimulated or primed with 10 μ M CDCA alone or in combination with 50 μ M 8.

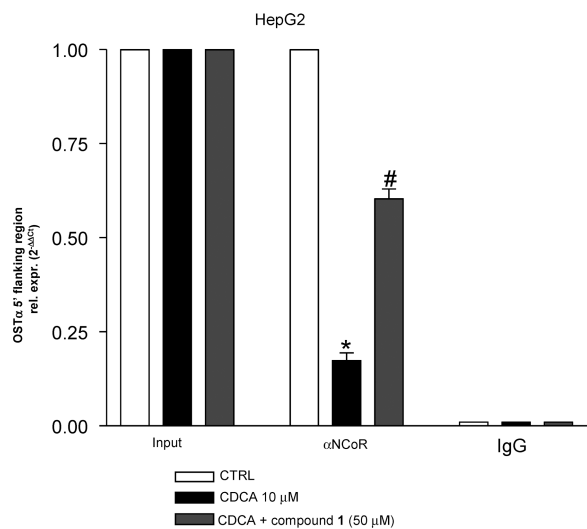


Figure 6. Chromatin immunoprecipitation shows that compound 8 antagonizes the effect of CDCA and stabilizes NCoR on the OST α promoter.

chromatin immunoprecipitation with an anti-NCoR antibody on HepG2 cells left untreated or primed with CDCA alone or in combination with compound 8. The binding of NCoR on immunoprecipitates was tested by real-time polymerase chain reaction (RT-PCR) using the canonical FXR responsive element expressed on the OST α promoter. As shown in Figure 6, in basal conditions, NCoR was constitutively bound on the OST α

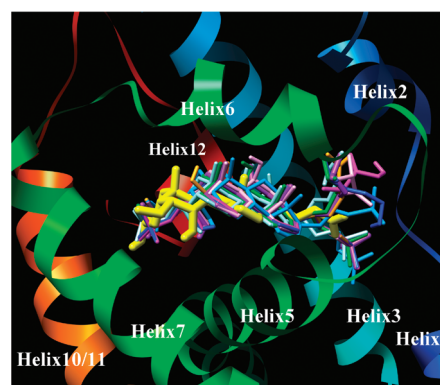


Figure 7. Superposition of 6-ECDCA (yellow) with compound 1 (green), 2 (violet), 3 (cyan), 4 (orange), 5 (light blue), 6 (pink), 7 (dark blue), and 8 (purple) in the canonical binding site of FXR (chain A of crystal structure 1OSV).

promoter. When FXR was activated by CDCA, the amount of NCoR bound to the OST α promoter was strongly down-regulated. This result is consistent with the recruitment of coactivators and with the activation of the gene transcription mediated by CDCA. Finally, in cells simultaneously treated with both CDCA and compound 8, NCoR was again recruited on the promoter, indicating that compound 8 prevents the dislodgment of the corepressor complex and the recruitment of the coactivators on the OST α promoter. Therefore, compound 8 exerts its antagonistic activity on FXR by stabilizing the NCoR complex, containing NCoR, on the promoters of FXR target genes, thus

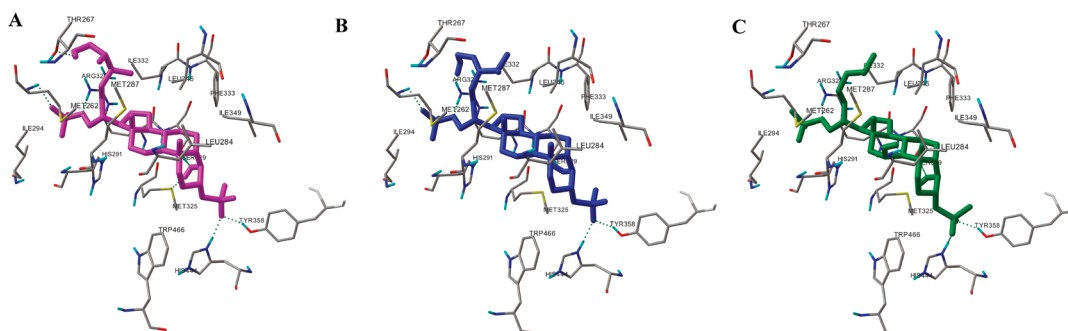


Figure 8. Three-dimensional models of docking pose of **8** (A, purple), **7** (B, dark blue), and **1** (C, green), with FXR (see the text for details).

preventing the recruitment of the transcription coactivator complex essential for transcription of these genes.

Docking Studies. To examine the crucial interactions involved in the binding mode of **8** to FXR at an atomic level, as well as to further clarify the effects exerted by the present series of marine steroids toward FXR, we ran a molecular docking simulation (Autodock Vina Software)³⁰ with compounds **1–8**. The relative positioning in the binding site of FXR⁴ of **1–8** with respect to 6-ECDCa is depicted in the Figure 7; as shown, the steric hindrance of the sulfate group at position 3 caused a general shift of the nucleus with respect to 6-ECDCa.

Nevertheless, for all of the docking complexes relative to compounds **1–8**, the sulfate group at position 3 was able to establish hydrogen bond contacts with three amino acids, crucial for the receptor activation⁴ (namely, Tyr358 in Helix 7, His444 in Helix 10/11, and Trp466 in Helix 12), while the sulfate group at position 21 was able to interact with the polar amino acids Arg328 of helix 5 and Met262 of helix 2 located at the entry of the pocket. For all of compounds **1–8**, the steroid nucleus accommodates the binding site (Figure 7), establishing hydrophobic interactions with the cavity pocket formed by Leu284, Met287, His291, Ile294 (helix 3), Met325, Ile332, Phe333 (helix 5), Leu345, and Ile349 (helix 6). Moreover, for all of the docking complexes, a hydrogen bond between the OH group of Ser329 (helix 5) side chain and the hydroxyl group at position 4 was evident. While the OH group at position 11 of **1**, **3**, and **6** interacted with the CO of Leu284, the carbonyl group at position 11 of **2**, the hydroxyl groups at position 12 of **3**, at position 5 of **4** and at position 2 of **5** did not show any interactions with the receptor.

In addition to the interactions reported above, the presence of a hydroxyl group at position 26 in compound **8** appeared to be critical for its FXR antagonistic activity, mainly for the involvement of this OH group in an additional hydrogen bond with Thr267 (Helix 2), as depicted in Figure 8A. Such an interaction was absent for compound **7**, where the OH at position 26 (Figure 8B) showed a hydrogen bond contact with Arg328, already involved in an interaction with the sulfate group at position 21.

The lack of simultaneous and efficient interactions—for all of our compounds—necessary for the stabilization of the active conformation of helix 12 and the loop H1–H2,⁴ may account for their inability to exert agonist activity, even competing with 6-ECDCa in occupying its binding site and so exhibiting antagonist activity.

In summary, here, we describe a novel class of FXR antagonists of marine origin. In addition to its value as a pharmacology tool,

an FXR antagonist might have a clinical utility. Indeed, results from mice harboring a disrupted FXR have shown that FXR deficiency protects against development of cholestasis, and it has been suggested that discovery of FXR antagonists might hold utility in the treatment of this condition. The present study describes the first FXR antagonist and grounds the basis for its exploitation in proof-of-concept studies in preclinical models of cholestasis. Despite the fact that compound **8** antagonizes FXR transactivation caused by CDCA in a concentration-dependent manner, it is increasingly recognized that BAs might activate additional receptors.^{6,7} TGR5 is a G protein-coupled seven transmembrane receptor activated by LCA and DCA but not by CDCA. However, it is highly unlikely that TGR5 mediates any of described activity of compound **8** for the following reasons. First of all, similarly to primary hepatocytes, HepG2 cells used in the present report lack the expression of TGR5. It is extensively reported that liver expression of TGR5 is very limited and that only nonparenchymal cells (that is, sinusoidal endothelial cells and resident macrophages, Kupffer cells) express the receptor.^{6,7} Second, to avoid interference by nongenomic effects, transactivation experiments were carried out using genes that express a canonical FXR responsive elements and that are induced or repressed by FXR in a promoter-dependent fashion. Third, TGR5 has no effect on BSEP, OST α , OST β , and Cyp7 α 1 expression in hepatocytes, and this fact excludes in principle that TGR5 might be involved in the reported effects.

Further in vivo studies aimed to establish the therapeutic potential of compound **8** were hampered by the scarcity of biological material available in our laboratories (8.7 mg). Indeed, compound **8** might become a standard probe in the field; therefore, its production in large scale represents a pressing target. Because the structural and stereochemistry complexity of the molecule makes its total synthesis quite difficult to perform, the planned large scale recollection of the shallow water *O. superba*, a common species along Japanese coasts, would afford a huge amount of biological material. Finally, the discovery of sulfated sterols as FXR antagonists reaffirms the utility of examining natural product libraries for identifying novel receptor ligands.

EXPERIMENTAL SECTION

HPLC was performed using a Waters model 510 pump equipped with Waters Rheodine injector and a differential refractometer, model 401. All sulfated sterols were isolated and purified as described in the cited references. The identity of each compound was secured by comparison of their NMR and MS data with those reported in the cited references. The purities of compounds **1–8** were determined to be greater than 95% by HPLC analysis on a C-18 column Macherey-Nagel Nucleodur

100-5 (5 μ , 250 mm \times 4.6 mm, 1.0 mL/min) using 45% MeOH/H₂O (isocratic mode) as eluent.

Plasmids, Cell Culture, Transfection, and Luciferase Assays. HepG2 cells were plated in a six-well plate at 5×10^5 cells/well. All transfections were made using Fugene HD transfection reagent (Roche). For the luciferase assay, HepG2 cells were transfected with 100 ng of pSG5-FXR, 100 ng of pSG5-RXR, and 200 ng of pCMV- β galactosidase and with 500 ng of the reporter vector p(hsp27)-TK-LUC containing the FXR response element IRI1 cloned from the promoter of heat shock protein 27 (hsp27). The pGEM vector (Promega) was added to normalize the amounts of DNA transfected in each well (2.5 μ g/well). At 48 h post-transfection, cells were stimulated for 18 h and then lysed in 100 μ L of diluted reporter lysis buffer (Promega), and 0.2 μ L of cellular lysates was assayed for luciferase activity using the Luciferase Assay System (Promega). Luminescence was measured using an automated luminometer. Luciferase activities were normalized for transfection efficiencies by dividing the relative light units by β -galactosidase activity expressed from cotransfected pCMV- β gal.

Quantitative RT-PCR. Fifty nanograms of template was added to the PCR mixture (final volume, 25 μ L) containing the following reagents: 0.2 μ M each primer and 12.5 μ L of 2X SYBR Green qPCR master mix (Invitrogen, Milan, Italy). All reactions were performed in triplicate, and the thermal cycling conditions were as follows: 2 min at 95 $^{\circ}$ C, followed by 40 cycles of 95 $^{\circ}$ C for 20 s, 55 $^{\circ}$ C for 20 s, and 72 $^{\circ}$ C for 30 s, in an iCycler iQ instrument (Biorad, Hercules, CA). The mean value of the replicates for each sample was calculated and expressed as the cycle threshold (C_T : cycle number at which each PCR reaction reaches a predetermined fluorescence threshold, set within the linear range of all reactions). The amount of gene expression was then calculated as the difference (ΔC_T) between the C_T value of the sample for the target gene and the mean C_T value of that sample for the endogenous control (GAPDH). Relative expression was calculated as the difference ($\Delta\Delta C_T$) between the ΔC_T values of the test sample and of the control sample (not treated) for each target gene. The relative quantitation value was expressed and shown as $2^{-\Delta\Delta C_T}$. All PCR primers were designed with PRIMER3-OUTPUT software using published sequence data from the NCBI database.

Chromatin Immunoprecipitation. HepG2 cells (10×10^6) were stimulated for 18 h with 10 μ M CDCA alone or with the combination of CDCA and 50 μ M compound 8. Cells left untreated received the vehicle alone (1% DMSO). At the end of the treatment, cells were cross-linked with 1% formaldehyde at room temperature for 10 min. The reaction was terminated by incubation with Glicine at a final condition of 125 mM for 5 min at room temperature. Cells were lysed in 500 μ L of Chip Lysis Buffer (1% SDS, 10 mM EDTA, and 50 mM Tris-HCl, pH 8), sonicated, and then pelleted at 13000 rpm for 1 min at 4 $^{\circ}$ C. The supernatant was collected, diluted with ChiP dilution buffer (0.01% SDS, 1% Triton X-100, 1.2 mM EDTA, pH 8, 16.7 mM Tris-HCl, pH 8, and 167 mM NaCl), and 20 μ g of chromatin was immunoprecipitated with an anti-NCoR antibody (upstate) or with an anti-IgG as negative control. Immunoprecipitates were collected with protein A beads (Amersham Bioscience) and washed sequentially, first with a low-salt wash buffer (0.1% SDS, 1% Triton X-100, 2 mM EDTA, pH 8, 20 mM Tris-HCl, pH 8, and 150 mM NaCl) and then with high-salt wash buffer (0.1% SDS, 1% Triton X-100, 2 mM EDTA, pH 8, 20 mM Tris-HCl, pH 8, and 500 mM NaCl). DNA was eluted with 500 μ L of elution buffer (1% SDS and 0.1 M NaHCO₃) for 30 min at 65 $^{\circ}$ C, and the cross-linking reactions were reversed by adding 20 μ L of 5 M NaCl by heating the mixture overnight at 65 $^{\circ}$ C. The DNA was recovered from immunoprecipitated material by proteinase K treatment at 65 $^{\circ}$ C for 1 h followed by phenol/chloroform (1:1) extraction and ethanol precipitation and dissolved into 50 μ L of water. Five microliters were used for quantitative RT-PCR of the OST α promoter with the following

sense and antisense primers: CTCTGGGAAGTCTAAAGTTCAG and CTCCTAAAGTCCAGTTCCTG.

Computational Details. Prior to docking calculations, full exploration of the conformational space of 1–8 was performed through molecular dynamics (MD) calculations at 300 K for 50 ns using the MMFFs force field (MacroModel software package)³¹ to give 100 structures (obtained by sampling every 500 ps), each of which was minimized using the Polak–Ribier conjugate gradient algorithm (PRCG, maximum derivative less than 0.05 kcal/mol). These calculations provided the lowest energy minimum conformer for 1–8.

Docking of the minimized energy structure of 1–8 to the crystal structure of the FXR bound to 6-ethyl-chenodeoxycholic acid was carried out with the Autodock Vina 1.0.3 software, considering an exhaustiveness value of 512, and adding to the Protein Data Bank (PDB) structure (accession code 1OSV)⁴ all of the polar hydrogens. For all of the docking studies, a grid box size of 26 $\text{Å} \times 26 \text{Å} \times 26 \text{Å}$, centered at coordinates 11.57 (x), 41.0 (y), and 15.496 (z) of the PDB structure, including all of the FXR surface, was used. All bonds of sulfated steroids 1–8 were treated as active torsional bonds, whereas the target was treated as rigid. Illustrations of the 3D model were generated using Chimera,³² Python.³³

AUTHOR INFORMATION

Corresponding Author

*Tel: (0039)081-678525. Fax (0039)081-678552. E-mail: angela.zampella@unina.it.

Author Contributions

^{||} Contributed equally to this work.

ABBREVIATIONS USED

BAs, bile acids; BSEP, bile salt export pump; CDCA, chenodeoxycholic acid; Cyp7a1, cytochrome; P450, family 7subfamily A, polypeptide; FXR, farnesoid-X-receptor; NCoR, nuclear corepressor; NRs, nuclear receptors; LBD, ligand-binding domain; OST α , organic solute transporter alpha; OST β , organic solute transporter beta; PDB, Protein Data Bank; PXR, pregnane-X-receptor; PXR E s, PXR response elements; RXR, retinoid-X-receptor; RT-PCR, real-time polymerase chain reaction

REFERENCES

- (1) Wang, H.; Chen, J.; Hollister, K.; Sowers, L. C.; Forman, B. M. Endogenous bile acids are ligands for the nuclear receptor FXR/BAR. *Mol. Cell* **1999**, *3*, 543–553.
- (2) Parks, D. J.; Blanchard, S. G.; Bledsoe, R. K.; Chandra, G.; Consler, T. G.; Kliewer, S. A.; Stimmel, J. B.; Willson, T. M.; Zavacki, A. M.; Moore, D. D.; Lehmann, J. M. Bile acids: Natural ligands for an orphan nuclear receptor. *Science* **1999**, *284*, 1365–1368.
- (3) Makishima, M.; Okamoto, A. Y.; Repa, J. J.; Tu, H.; Learned, R. M.; Luk, A.; Hull, M. V.; Lustig, K. D.; Mangelsdorf, D. J.; Shan, B. Identification of a nuclear receptor for bile acids. *Science* **1999**, *284*, 1362–1365.
- (4) Mi, L.-Z.; Devarakonda, S.; Harp, J. M.; Han, Q.; Pellicciari, R.; Willson, T. M.; Khorasanizadeh, S.; Rastinejad, F. Structural Basis for Bile Acid Binding and Activation of the Nuclear Receptor FXR. *Mol. Cell* **2003**, *11*, 1093–1100.
- (5) Fiorucci, S.; Mencarelli, A.; Distrutti, E.; Palladino, G.; Cipriani, S. Targeting farnesoid-X-receptor: from medicinal chemistry to disease treatment. *Curr. Med. Chem.* **2010**, *17*, 139–159.
- (6) Fiorucci, S.; Cipriani, S.; Baldelli, F.; Mencarelli, A. Bile acid-activated receptors in the treatment of dyslipidemia and related disorders. *Prog. Lipid Res.* **2010**, *49*, 171–185.

- (7) Fiorucci, S.; Mencarelli, A.; Palladino, G.; Cipriani, S. Bile-acid-activated receptors: Targeting TGR5 and farnesoid-X-receptor in lipid and glucose disorders. *Trends Pharmacol. Sci.* **2009**, *30*, 570–580.
- (8) Fiorucci, S.; Baldelli, F. Farnesoid X receptor agonists in biliary tract disease. *Curr. Opin. Gastroenterol.* **2009**, *25*, 252–259.
- (9) Fiorucci, S.; Rizzo, G.; Donini, A.; Distrutti, E.; Santucci, L. Targeting farnesoid X receptor for liver and metabolic disorders. *Trends Mol. Med.* **2007**, *13*, 298–309.
- (10) Pellicciari, R.; Fiorucci, S.; Camaioni, E.; Clerici, C.; Costantino, G.; Maloney, P. R.; Morelli, A.; Parks, D. J.; Willson, T. M. 6 α -Ethylchenodeoxycholic acid (6-ECDC), a potent and selective FXR agonist endowed with anticholestatic activity. *J. Med. Chem.* **2002**, *45*, 3569–3572.
- (11) Nicolaou, K. C.; Evans, R. M.; Roecker, A. J.; Hughes, R.; Downes, M.; Pfefferkorn, J. A. Discovery and optimization of non-steroidal FXR agonists from natural product-like libraries. *Org. Biomol. Chem.* **2003**, *1*, 908–920.
- (12) Dussault, L.; Beard, R.; Lin, M.; Hollister, K.; Chen, J.; Xiao, J.-H.; Chandraratna, R.; Forman, B. M. Identification of gene-selective modulators of the bile acid receptor FXR. *J. Biol. Chem.* **2003**, *278*, 7027–7033.
- (13) Maloney, P. R.; Parks, D. J.; Haffner, C. D.; Fivush, A. M.; Chandra, G.; Plunket, K. D.; Creech, K. L.; Moore, L. B.; Wilson, J. G.; Lewis, M. C.; Jones, S. A.; Willson, T. M. Identification of a chemical tool for the orphan nuclear receptor FXR. *J. Med. Chem.* **2000**, *43*, 2971–2974.
- (14) Singh, R. B.; Niaz, M. A.; Ghosh, S. Hypolipidemic and antioxidant effects of *Commiphora mukul* as an adjunct to dietary therapy in patients with hypercholesterolemia. *Cardiovasc. Drugs Ther.* **1994**, *4*, 659–664.
- (15) Sinal, C. J.; Gonzalez, F. J. Guggulsterone: an old approach to a new problem. *Trends Endocrinol. Metab.* **2002**, *13*, 275–276.
- (16) Nozawa, H. Xanthohumol, the chalcone from beer hops (*Humulus lupulus* L.), is the ligand for farnesoid X receptor and ameliorates lipid and glucose metabolism in KK-Ay mice. *Biochem. Biophys. Res. Commun.* **2005**, *336*, 754–761.
- (17) Nam, S.-J.; Ko, H.; Shin, M.; Ham, J.; Chin, J.; Kim, Y.; Kim, H.; Shin, K.; Choi, H.; Kang, H. Farnesoid X-activated receptor antagonists from a marine sponge *Spongia* sp. *Bioorg. Med. Chem. Lett.* **2006**, *16*, 5398–5402.
- (18) Urizar, N. L.; Liverman, A. B.; Dodds, D. T.; Silva, F. V.; Ordentlich, P.; Yan, Y.; Gonzalez, F. J.; Heyman, R. A.; Mangelsdorf, D. J.; Moore, D. D. A natural product that lowers cholesterol as an antagonist ligand for FXR. *Science* **2002**, *296*, 1703–1706.
- (19) Wu, J.; Xia, C.; Meier, J.; Li, S.; Hu, X.; Lala, D. S. The hypolipidemic natural product guggulsterone acts as an antagonist of the bile acid receptor. *Mol. Endocrinol.* **2002**, *16*, 1590–1597.
- (20) Cui, J.; Huang, L.; Zhao, A.; Lew, J. L.; Sahoo, S.; Meinke, P. T. Guggulsterone is a farnesoid X receptor antagonist in coactivator association assays but acts to enhance transcription of bile salt export pump. *J. Biol. Chem.* **2003**, *278*, 10214–10220.
- (21) Burris, T. P.; Montrose, C.; Houck, K. A.; Osborne, H. E.; Bocchinfuso, W. P.; Yaden, B. C.; Cheng, C. C.; Zink, R. W.; Barr, R. J.; Hepler, C. D.; Krishnan, V.; Bullock, H. A.; Burris, L. L.; Galvin, R. J.; Bramlett, K.; Stayrook, K. R. The hypolipidemic natural product guggulsterone is a promiscuous steroid receptor ligand. *Mol. Pharmacol.* **2005**, *67*, 948–954.
- (22) McKee, T. C.; Cardellina, J. H. II; Riccio, R.; D'Auria, M. V.; Iorizzi, M.; Minale, L.; Moran, R. A.; Gulakowski, R. J.; McMahon, J. B.; Buckheit, R. W., Jr.; Snader, K. M.; Boyd, M. R. HIV-inhibitory natural products. 11. Comparative studies of sulfated sterols from marine invertebrates. *J. Med. Chem.* **1994**, *37*, 793–797.
- (23) Roccatagliata, A. J.; Maier, M. S.; Seldes, A. M.; Pujol, C. A.; Damonte, E. B. Antiviral sulfated steroids from the ophiuroid *Ophioplocus januarii*. *J. Nat. Prod.* **1996**, *59*, 887–889.
- (24) Roccatagliata, A. J.; Maier, M. S.; Seldes, A. M. New sulfated polyhydroxysteroids from the antarctic ophiuroid *Astrotoma agassizii*. *J. Nat. Prod.* **1998**, *61*, 370–374.
- (25) Comin, M. J.; Maier, M. S.; Roccatagliata, A. J.; Pujol, C. A.; Damonte, E. B. Evaluation of the antiviral activity of natural sulfated polyhydroxysteroids and their synthetic derivatives and analogs. *Steroids* **1999**, *64*, 335–340.
- (26) Fu, X.; Schmitz, F. J.; Lee, R. H.; Papkoff, J. S.; Slate, D. L. Inhibition of protein tyrosine kinase pp60v-src: Sterol sulfates from the brittle star *Ophiarachna incrassata*. *J. Nat. Prod.* **1994**, *57*, 1591–1594.
- (27) Riccio, R.; D'Auria, M. V.; Minale, L.; La Barre, S.; Pusset, J. Novel marine steroid sulfates from Pacific ophiuroids. *J. Org. Chem.* **1987**, *52*, 3947–3952.
- (28) Riccio, R.; D'Auria, M. V.; Minale, L. Unusual sulfated marine steroids from the ophiuroid *Ophioderma longicaudum*. *Tetrahedron* **1985**, *41*, 6041–6046.
- (29) D'Auria, M. V.; Riccio, R.; Uriarte, E.; Minale, L.; Tanaka, J.; Higa, I. Isolation and structure elucidation of seven new polyhydroxylated sulfated sterols from the ophiuroid *Ophiopsis superba*. *J. Org. Chem.* **1989**, *54*, 234–239.
- (30) Trott, O.; Olson, A. J. Improving the speed and accuracy of docking with a new scoring function, efficient optimization, and multi-threading. *J. Comput. Chem.* **2010**, *31*, 455–461.
- (31) Mohamadi, F.; Richards, N. G.; Guida, W. C.; Liskamp, R.; Lipton, M.; Caufield, C.; Chang, G.; Hendrickson, T.; Still, W. C. Macromodel—an integrated software system of modelling organic and bioorganic molecules using molecular mechanics. *J. Comput. Chem.* **1990**, *11*, 440–467.
- (32) Pettersen, E. F.; Goddard, T. D.; Huang, C. C.; Couch, G. S.; Greenblatt, D. M.; Meng, E. C.; Ferrin, T. E. UCSF Chimera—A visualization system for exploratory research and analysis. *J. Comput. Chem.* **2004**, *25*, 1605–1612.
- (33) Sanner, M. F. Python: A Programming Language for Software Integration and Development. *J. Mol. Graphics Modell.* **1999**, *17*, 57–61.